Published online 6 February 2015 *Nucleic Acids Research, 2015, Vol. 43, No. 4* **2313–2325**
doi: 10.1093/nar/gkv034

Viroid RNA turnover: characterization of the subgenomic RNAs of potato spindle tuber viroid accumulating in infected tissues provides insights into decay pathways operating *in vivo*

Sofia Minoia[1], Beatriz Navarro[2], Sonia Delgado[1], Francesco Di Serio[2,*] and Ricardo Flores[1,*]

[1]Instituto de Biología Molecular y Celular de Plantas (IBMCP), Universidad Politécnica de Valencia-Consejo Superior de Investigaciones Científicas, Valencia, Spain and [2]Istituto per la Protezione Sostenibile delle Piante, UOS Bari, Consiglio Nazionale delle Ricerche, Bari, Italy

Received February 21, 2014; Revised December 16, 2014; Accepted January 09, 2015

ABSTRACT

While biogenesis of viroid RNAs is well-known, how they decay is restricted to data involving host RNA silencing. Here we report an alternative degradation pathway operating on potato spindle tuber viroid (PSTVd), the type species of nuclear-replicating viroids (family *Pospiviroidae).* Northern-blot hybridizations with full- and partial-length probes revealed a set of PSTVd (+) subgenomic (sg)RNAs in early-infected eggplant, some partially overlapping and reaching levels comparable to those of the genomic circular and linear forms. Part of the PSTVd (+) sgRNAs were also observed in *Nicotiana benthamiana* (specifically in the nuclei) and tomato, wherein they have been overlooked due to their low accumulation. Primer extensions of representative (+) sgRNAs failed to detect a common 5′ terminus, excluding that they could result from aborted transcription initiated at one specific site. Supporting this view, 5′- and 3′-RACE indicated that the (+) sgRNAs have 5′-OH and 3′-P termini most likely generated by RNase-mediated endonucleolytic cleavage of longer precursors. These approaches also unveiled PSTVd (−) sgRNAs with features similar to their (+) counterparts. Our results provide a mechanistic insight on how viroid decay may proceed *in vivo* during replication, and suggest that synthesis and decay of PSTVd strands might be coupled as in mRNA.

INTRODUCTION

Viroids are a singular class of subviral replicons just composed by a small (around 250–400 nt) single-stranded RNA with circular structure and compact folding that results from extensive self-complementarity (1–4). Considering their structural and functional features, viroids have been assigned to two families: (i) *Pospiviroidae,* including those that adopt a rod-like secondary structure with a central conserved region, and replicate in the nucleus through an asymmetric rolling-circle mechanism catalyzed by host enzymes (5–7), and (ii) *Avsunviroidae* comprising those with a quasi-rod-like or clearly branched secondary structure, and with replication in plastids (mostly chloroplasts) through a symmetric rolling-circle mechanism catalyzed by host enzymes and viroid-embedded hammerhead ribozymes (8–10). A significant portion of past and recent investigations on viroids has been focused on potato spindle tuber viroid (PSTVd), the type species of the family *Pospiviroidae* and the first that was discovered, characterized structurally and sequenced (11–14), which has thus become a model system. The picture that has emerged from numerous studies on the biosynthesis (replication) of PSTVd and closely-related viroids is fairly complete. The RNA polymerase II, redirected to accept RNA templates, transcribes reiteratively the infecting monomeric circular RNA—arbitrarily attributed the (+) polarity—into multimeric complementary (−) strands, which are the templates for a second RNA–RNA transcription catalyzed by the same enzyme that results into multimeric (+) strands (15–18). The latter are cleaved into unit-length forms, presumably by a class III RNase (19,20), and then circularized by DNA ligase I redirected to accept RNA substrates (21). The finding by *in situ* hybridization of PSTVd (+) strands in the nucleolus and nucleoplasm, but of (−) strands only in the nucleoplasm (22), is consistent with RNA polymerization taking place in this latter compartment, while processing of the (+) strands would occur in the nucleolus wherein the precursors of rRNAs and tRNAs are also processed (23).

*To whom correspondence should be addressed. Tel: +34 963877861; Fax: +34 963877859; Email: rflores@ibmcp.upv.es
Correspondence may also be addressed to Francesco Di Serio. Tel: +39 0805443071; Fax: +39 0805442911; Email: f.diserio@ba.ivv.cnr.it

Viroid accumulation, however, is determined by the balance between replication (transcription and processing) and degradation, with the progress achieved in understanding replication having not been matched with that on viroid decay. This case is not specific for viroids because whereas transcription has been extensively studied for mRNAs—one the most in-depth analyzed classes of cellular RNAs—little is still known on regulation of mRNA degradation and its coupling with transcription (24,25); only very recently it has been shown that mRNA transcription and decay are linked through common factors (26). The accumulation in tissues infected by members of the two families of viroid-derived small RNAs (vd-sRNAs) with the typical properties of the sRNAs generated by dicer-like enzymes (DCLs) (27–31), clearly indicates that viroids are targeted by this first RNA silencing defensive barrier raised by the host against invading RNAs (32,33). Moreover, the subsequent loading of PSTVd-sRNAs on different Argonaute (AGO) proteins and their attenuating effects observed on PSTVd titer (34), supports the view that viroids are also targeted by the second RNA silencing defensive barrier of the host: the RNA induced silencing complex (RISC), the core of which is invariably formed by one member of the AGO family (35–37). It is likely that other degradation routes may also act on viroid RNAs, but the available information is essentially restricted to: (i) the increase in PSTVd-infected tomato of some nucleolytic activities that have been linked to symptom appearance rather than to viroid RNA degradation (38), and (ii) the accumulation in immature pollen from hop plants infected by hop latent viroid (family *Pospiviroidae)* of viroid RNA fragments (100 to 230 nt) that were not further characterized and have been associated with developmentally activated nucleases (39).

In the course of our studies on PSTVd infection in different solanaceous hosts, we have consistently observed in eggplant a pattern of viroid subgenomic RNAs (sgRNAs) accompanying the monomeric circular *(mc)* and linear *(ml)* forms. Molecular analysis of the PSTVd-sgRNAs, including their size and terminal groups, has expanded our view upon how viroid decay occurs.

MATERIALS AND METHODS

Host plants and viroid source

Seedlings from eggplant *(Solanum melongena* L.) cv. 'Black beauty', *Nicotiana benthamiana,* and tomato *(S. lycopersicum* L.) cv. 'Rutgers', were maintained in a growth chamber (28°C with fluorescent light for 16 h and 25°C in darkness for 8 h). At the cotyledon/first true leaf stage they were mock- or viroid-inoculated by: (i) agroinfiltration (eggplant and *N. benthamiana*) with cultures of *Agrobacterium tumefaciens* C58 carrying a binary plasmid with a head-to-tail dimeric insert of PSTVd (NB variant, GenBank accession number AJ634596.1) under the control of the 35S promoter of cauliflower mosaic virus (40), or (ii) mechanically (tomato) with an RNA preparation from tissue infected with the same PSTVd strain.

RNA extraction and northern-blot hybridization

Total leaf nucleic acid preparations, obtained by double extraction with buffer-saturated phenol, were ethanol-precipitated, resuspended and separated by denaturing polyacrylamide gel electrophoresis (PAGE) (in 1X TBE buffer and 8 M urea) on either 5% gels (for unit-length and sgRNAs) or 17% gels (for vd-sRNAs) and stained with ethidium bromide. Equal loading was assessed by the fluorescence emitted by the 5S RNA. Following electrotransference of RNAs to Hybond-N+ membranes (Roche Diagnostics GmbH), they were hybridized with internally radiolabeled full-length riboprobes (synthesized by *in vitro* transcription) for detecting PSTVd (+) and (−) strands, or with 5′-radiolabeled deoxyribonucleotide probes (prepared with T4 polynucleotide kinase (PK) (Roche Diagnostics GmbH) and [γP^{32}]-ATP, 3000 Ci/mmol, Perkin Elmer) complementary to specific regions of the PSTVd (+) RNA (Supplementary Table S1). Radiolabeling of the probes was according to standard procedures (41). Hybridization was at 70°C in the presence of 50% formamide (for detecting the *mc* and *ml* forms and the sgRNAs with full-length riboprobes), or at 42°C with PerfectHyb Plus hybridization buffer (Sigma) (for detecting *mc* and *ml* forms and the sgRNAs with the deoxyribonucleotide probes, and vd-sRNAs with a full-length riboprobe) (42). After washing at 60°C in 0.1X SSC with 0.1% SDS (for unit-length and sgRNAs), or at 55°C in 1X SSC with 0.1% SDS (for vd-sRNAs), the membranes were analyzed with a phosphoimager (Fujifilm FLA-5100) using programs Image Reader FLA-5100 and Image Gauge 4.0.

Primer extension analysis

Chemically-synthesized primers (Fisher Scientific) were purified as indicated previously (43). PSTVd *ml* forms and sgRNAs were gel-eluted overnight at 37°C with Tris-HCl 10 mM, pH 7.5 containing 1 mM EDTA and 0.1% SDS, and recovered by ethanol precipitation. The 5′ termini of the purified RNAs were determined by primer extension catalyzed by reverse transcriptase (SuperScript II RNase H^-; Invitrogen) as reported before (44) with the exception that primers (Supplementary Table S2) were previously 5′-labeled as indicated above. The extension products were run in 6% sequencing polyacrylamide gels in parallel with four sequencing ladders, generated by T7 DNA polymerase-catalyzed extensions of the same 5′-radiolabeled primers in reaction mixtures containing a recombinant plasmid with a full-length PSTVd-cDNA insert and mixtures of deoxy and dideoxy nucleoside triphosphates (NTPs) (Sequenase version 2.0 DNA sequencing kit, USB, Affimetrix, Inc).

RNA ligase-mediated rapid amplification of 5′ cDNA ends (RLM-RACE)

Unless otherwise stated, two aliquots of each gel-purified RNA, one pretreated with PK and ATP (41), and the other untreated, were fused to an RNA adaptor (5′-CGACUGGAGCACGAGGACACUGACAUGG ACUGAAGGAGUAGAAA-3′) using T4-RNA ligase 1 (Epicentre) and ATP in the buffer recommended by the supplier (Roche Diagnostics GmbH) as previously described (44). When using as control a full-length PSTVd (−) *in*

vitro transcript with 5′-triphosphorylated and 3′-hydroxyl termini, one aliquot was left untreated while the other was treated with RNA 5′ polyphosphatase (PP) (Epicentre) to convert the 5′-triphosphorylated group into a 5′-monophosphorylated group. The ligation products were reverse transcribed with suitable PSTVd-specific primers, and then polymerase chain reaction (PCR)-amplified with an adapter-specific primer and viroid-specific primers internal with respect to the preceding ones (Supplementary Table S3), using the Expand High Fidelity DNA polymerase in the buffer recommended by the supplier (Roche Diagnostics GmbH) (44). After an initial denaturation at 94°C for 2 min, the amplification profile consisted of 30 cycles at 94°C for 30 s, 58 to 72°C for 30 s and 72°C for 2 min. Following non-denaturing PAGE (in TAE buffer) in 5% gels, those amplicons of expected length were eluted, cloned and sequenced with a ABI 3100 XL (Life Technologies) apparatus.

PolyA-mediated rapid amplification of 3′ cDNA ends (3′-RACE)

Two aliquots of the gel-purified RNAs of interest, one pretreated with alkaline phosphatase (AP) (Roche Diagnostics GmbH) and the other untreated, were polyadenylated with yeast poly(A) polymerase (USB, Affimetrix, Inc) and ATP following the conditions recommended by the supplier. The polyadenylated products were reverse transcribed with a polyA tail-complementary primer (5′-CCGGATCCTCTAGATCGGCCGCT$_{17}$V-3′, where V is A, C or G) (20), and subjected to PCR amplification with this same primer and PSTVd-specific primers derived from the corresponding sgRNAs. After an initial denaturation at 94°C for 2 min, the amplification profile consisted of 38 cycles at 94°C for 30 s, 63 to 68°C for 30 s and 72°C for 2 min. Following non-denaturing PAGE in 5% gels, those amplicons of expected length were eluted, cloned and sequenced as indicated above.

Isolation of nuclei

PSTVd-infected leaves (5 g) of *N. benthamiana* were processed as reported previously (45) with some modifications. In brief, they were ground with liquid nitrogen to a fine powder and resuspended in five volumes of ice-cold nuclear isolation buffer (NIB): 10 mM MES-KOH pH 5.4, 10 mM NaCl, 10 mM KCl, 2.5 mM EDTA, 250 mM sucrose, 0.1 mM spermine, 0.5 mM spermidine and 1 mM DTT. The homogenate was filtered through two layers of cheesecloth and one of Miracloth, and Triton X-100 (10%) was added dropwise until a final concentration of 0.5%. After incubation for 20 min at 4°C with gentle agitation, the suspension was centrifuged at 1000 g for 10 min at 4°C. The white pellet containing the crude nuclear preparation was slowly resuspended in 1 ml of NIB, loaded on top of a 1.3 ml cushion of 2.5 M sucrose in NIB, and centrifuged at 12 000 g for 10 min. The pellet of purified nuclei was washed twice by resuspension in 1 ml of NIB and centrifugation at 1000 g for 5 min, and their integrity was assessed by 4′,6-diamidino-2-phenylindole (DAPI) staining and observation with a fluorescence microscope.

RESULTS

An unexpected finding: PSTVd (+) sgRNAs of precise size accumulate to high levels in early infectious stages in eggplant

Since the very initial research on viroids, most studies on PSTVd have been performed using tomato because this experimental host is easy to grow in the greenhouse, reacts to intermediate and severe PSTVd strains with clear symptoms in about two weeks, and accumulates relatively high titers of the agent (46). More recently, some studies have focused on *N. benthamiana* (38,42,47–48), regarded as a model host in plant virology given that it allows replication of a wide array of viruses and certain viroids including PSTVd—possibly as a consequence of being deficient in at least one RNA silencing antiviral pathway (49)—and that it is particularly appropriate for agroinfiltration experiments (50). Lately, we have also become interested in eggplant, which like the other two preceding species belongs to the family *Solanaceae,* given that it is one of the few plants able to sustain replication of members of the two viroid families, PSTVd (51) and eggplant latent viroid (ELVd) (52), a feature convenient for comparative studies. In contrast to ELVd, which as reflected in its name replicates symptomlessly, we have observed a stunted phenotype in PSTVd-infected eggplant (data not shown), in agreement with a previous report (51).

In an attempt to follow the progress of PSTVd accumulation in eggplant inoculated by agroinfiltration, which induces a more efficient and reproducible infection, we examined at different time intervals nucleic acid preparations by denaturing PAGE and northern-blot hybridization with a radioactive riboprobe for detecting PSTVd (+) strands. The PSTVd (+) *mc* and linear *(ml)* genomic forms were observed in upper non-inoculated leaves 15 days post-inoculation (dpi); intriguingly, a set of accompanying 6–8 viroid sgRNAs were also visible, with the intensity of some of their signals being similar or even higher than those generated by the *mc* and *ml* forms (Figure 1). The clear band definition, as opposed to a smear, excluded that the PSTVd (+) sgRNAs could emerge from non-specific degradation; moreover, their absence in a preparation from non-infected eggplant artificially supplemented with purified PSTVd *mc* forms (Figure 2), dismissed the possibility that these sgRNAs could be generated *in vitro* during extraction (in contrast to the *ml* forms resulting from artifactual single nicks introduced in the *mc* form). A band profile essentially identical to that observed in eggplant leaves at 15 dpi was obtained when leaves of a similar developmental stage were collected from the same infected plants at 20 and 25 dpi, but with a quantitative difference: the relative intensity of the *mc* and *ml* bands increased with time (Figure 1). This difference was even more pronounced in another experiment where we also examined the intensity of vd-sRNA bands, which paralleled that of the *mc* and *ml* forms (Supplementary Figure S1) in consonance with previous results (38,42,53–54). To check whether these PSTVd-sgRNAs were idiosyncratic for eggplant, we applied the same analytic procedure to nucleic acid preparations from *N. benthamiana* and tomato leaves taken at similar time intervals: at least some of the lower-than-unit-length bands were observed co-migrating with those of eggplant, but with

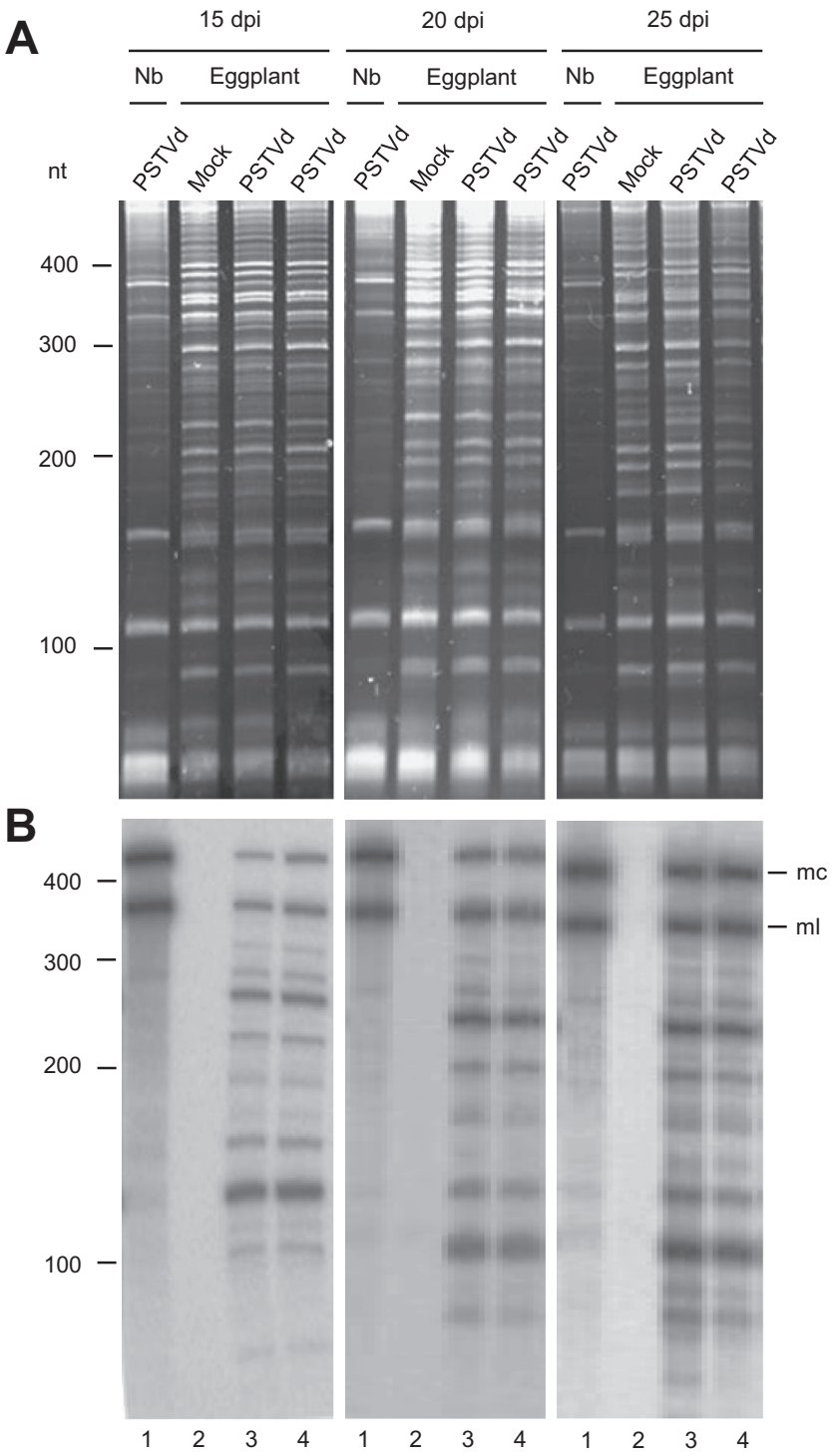

Figure 1. Infection of eggplant by PSTVd results in the accumulation of a series of PSTVd (+) sgRNAs accompanying the genomic *mc* and *ml* (+) forms. Total RNAs from upper non-inoculated leaves collected at 15, 20 and 25 dpi were separated by denaturing PAGE in 5% gels and revealed with ethidium bromide **(A),** and by northern-blot hybridization with a radiolabeled riboprobe for detecting PSTVd (+) strands **(B)**. In each panel lane 1 corresponds to PSTVd-infected *N. benthamiana,* lane 2 to mock-inoculated eggplant, and lanes 3 and 4 to PSTVd-infected eggplant. Positions of RNA markers (in nt) are indicated on the left, and those of the PSTVd *mc* and ml forms on the right.

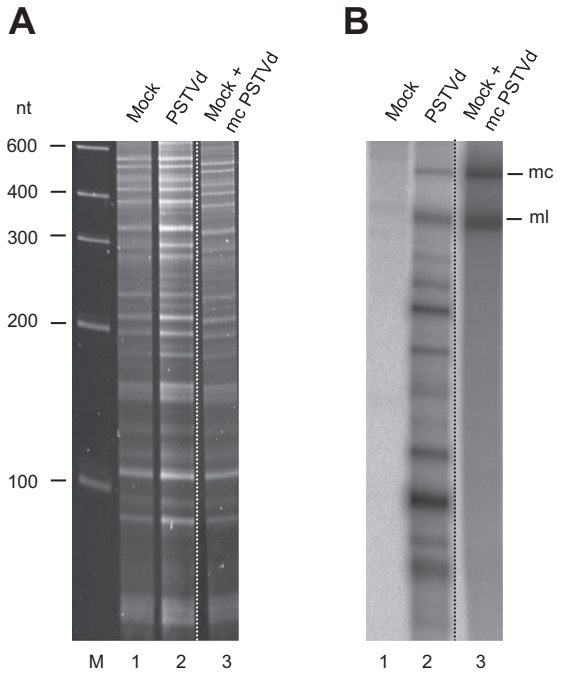

Figure 2. PSTVd (+) sgRNAs are not artifacts generated during *in vitro* extraction. Total RNAs were separated by denaturing PAGE in 5% gels and revealed with ethidium bromide **(A),** and by northern-blot hybridization with a radiolabeled riboprobe for detecting PSTVd (+) strands **(B)**. Lane M, RNA markers; lanes 1, mock-inoculated eggplant; lanes 2, PSTVd-infected eggplant; lanes 3, mock-inoculated eggplant supplemented before extraction with PSTVd *mc* forms from infected tissue. Positions of RNA markers (in nt) are indicated on the left, and those of the *mc* and *ml* forms on the right.

a significant lesser intensity in most cases; the intensity of the *mc* forms, however, was higher in *N. benthamiana* and tomato than in eggplant (Figure 3).

Moreover, we also examined the agroinfiltrated leaves of *N. benthamiana* at 4, 6 and 8 dpi. Interestingly, the PSTVd-sgRNAs became even more apparent than in the upper non-inoculated leaves—particularly when comparing the intensity of their bands with that of the *mc* and *ml* forms—possibly because the primary PSTVd dimeric transcript also served as a precursor of the PSTVd-sgRNAs (Supplementary Figure S2). Altogether these results disclosed that, besides the *mc* and *ml* forms upon which most of the attention has been previously focused, PSTVd infection gives also rise to a series of (+) sgRNAs that have been overlooked so far since, in contrast to eggplant, they accumulate in other solanaceous hosts like *N. benthamiana* and tomato at relatively low levels. We assumed that determining where the sgRNAs come from and how they are generated might provide some valuable *in vivo* insights into PSTVd synthesis or degradation, because at this stage we could not discriminate from which of these two major routes the (+) sgRNAs resulted from.

Delimiting the PSTVd (+) RNA regions from which the sgRNAs originate

To get a first outlook about where the sgRNAs map on the genomic PSTVd (+) RNA, we next examined eggplant nucleic acid preparations by denaturing PAGE and northern-blot hybridization with six 5′-radiolabeled oligodeoxyribonucleotide probes complementary to different segments of the full-length PSTVd (+) RNA: three (probes I to III) derived from the lower strand of the rod-like secondary structure and the other three (probes IV to VI) from the upper strand (Supplementary Table S1 and Figure S3A). As anticipated, all probes hybridized—with different intensity—with the *mc* and *ml* RNAs from the preparations of infected eggplant and *N. benthamiana.* However, this was not the case with the (+) sgRNAs. For instance, of the five sgRNAs selected for further characterization (see below), probe II hybridized strongly with sgRNA 5, while probes IV and V hybridized strongly with sgRNAs 1 and 3 (Supplementary Figure S3B). Although these data should be interpreted with care due to the low temperature used for hybridization (42°C), collectively they indicated that the sgRNAs come from different regions of the genomic PSTVd (+) RNA, and that some of them could be partially overlapping or even form part of others.

To better define their properties, five (+) sgRNAs (1 to 5) were eluted from denaturing polyacrylamide gels and their purity re-assessed by denaturing PAGE and northern-blot hybridization with the full-length riboprobe (Supplementary Figure S4); the *ml* forms were also similarly recovered and used as an additional control. Each of these purified RNAs served as templates in independent reverse transcriptase-catalyzed extensions of two appropriate 5′-radiolabeled primers, either corresponding to some of the probes indicated above or newly designed (Supplementary Table S2). Running the primer extension products in long denaturing 6% sequencing gels in parallel with four sequencing ladders—obtained with the same primer and a recombinant plasmid with a complete PSTVd-cDNA insert—resulted in the identification of the following 5′ termini: U296 (sgRNAs 1 and 3), G72 (sgRNA 2), C13 (sgRNA 4) and G201 (sgRNA 5) (Figure 4). These termini—together with the estimated size of the sgRNAs inferred from their mobility in denaturing polyacrylamide gels—were consistent with results from the hybridization experiments using the specific probes reported above, as also was the observation that sgRNAs 1 and 3 have the same 5′ termini (thus denoting that the latter is contained in the former). Although this finding might be interpreted as the sgRNAs 3 resulting from premature transcription termination of the sgRNAs 1, the lack of a 5′ terminus common for the five (+) sgRNAs and other additional evidence (see below), excluded this possibility. Inspection of the positions where the 5′ termini of the sgRNAs map in the rod-like secondary structure of PSTVd (+) RNA did not reveal any clear preference for loops or double-stranded segments (Figure 4). Interestingly, extension of the *ml* RNA generated a clear stop at G96 (Figure 4), in agreement with previous results indicating that this is the cleavage site *in vitro* (55) and *in vivo* (19,20) of the oligomeric (+) strands of PSTVd and other representative members of the family *Pospiviroidae*.

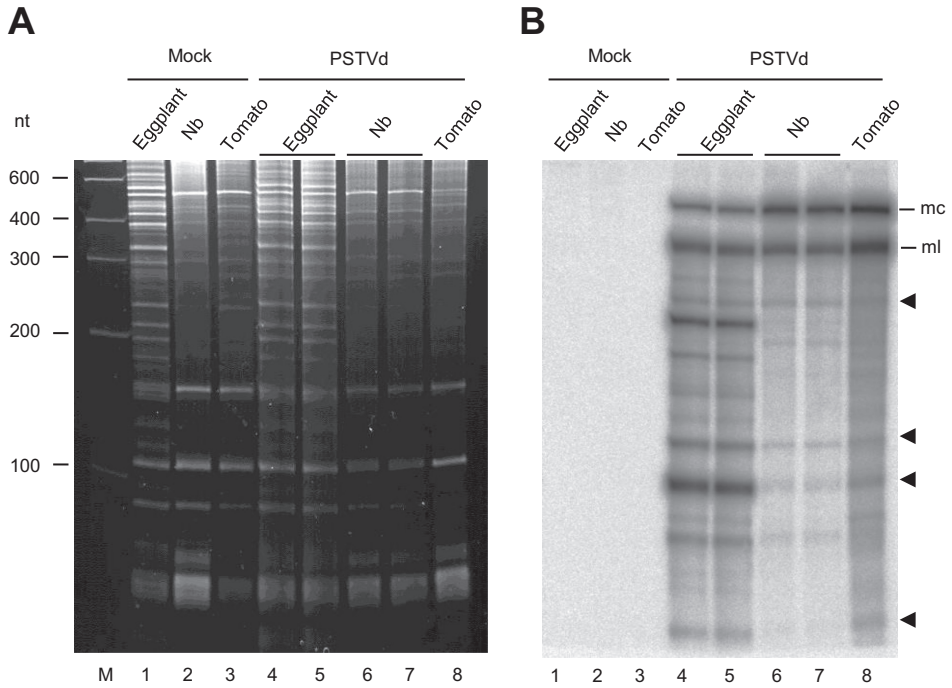

Figure 3. Accumulation in three different hosts of PSTVd (+) *mc*, *ml* and sgRNAs. Total RNAs from upper non-inoculated leaves were separated by denaturing PAGE in 5% gels and revealed with ethidium bromide **(A),** and by northern-blot hybridization with a radiolabeled riboprobe for detecting PSTVd (+) strands **(B)**. Lanes 1 to 3, mock-inoculated controls of eggplant, *N. benthamiana* and tomato, respectively. Lanes 4 to 8, PSTVd-infected eggplant (lanes 4 and 5), *N. benthamiana* (lanes 6 and 7) and tomato (lane 8). Loading was equalized by the intensity of the 5S RNA stained with ethidium bromide (not shown). Positions of the PSTVd (+) *mc* and *ml* forms are indicated on the right and those of RNA markers (in nt) on the left. Arrowheads mark some PSTVd (+) sgRNAs common to the three hosts. Leaves were collected at similar time intervals (20–25 dpi).

The terminal groups of the PSTVd (+) sgRNAs reveal that they do not result from aborted transcription but from endonucleolytic cleavage of longer viroid RNAs

To obtain further independent evidence for the 5′ termini of the sgRNAs, we applied a 5′ RNA ligase-mediated rapid amplification of cDNA ends (RLM-RACE). When implemented with proper modifications, this approach provides additional data about the chemical groups of these termini, from which their origin can be inferred (44). More specifically, we examined in this respect the (+) sgRNAs 1 to 5, using as a control the PSTVd (+) *ml* form—delimited by positions C1 and G2 with 5′-hydroxyl and 2′,3′-cyclic phosphodiester termini, respectively—resulting from self-cleavage of a full-length *in vitro* transcript flanked by hammerhead and hepatitis delta virus ribozymes (21).

To characterize their corresponding 5′ termini, the RNAs were eluted from denaturing polyacrylamide gels and two aliquots of each were ligated to an RNA adaptor using T4 RNA ligase 1, which demands 5′-P and 3′-OH termini; one aliquot was pretreated with T4 PK and ATP (to phosphorylate 5′-OH termini) while the other remained untreated. The resulting ligation products were reverse transcribed with appropriate PSTVd-specific primers (in some instances the same used before as probes), and PCR-amplified with an adapter-specific primer and viroid-specific primers internal with respect to the previous ones (Supplementary Table S3). PCR products were fractionated by non-denaturing PAGE and those of the expected size cloned and sequenced. The amplification product containing the terminus predicted for the PSTVd (+) *ml* forms generated *in vitro* was only observed in the PK-pretreated aliquot, thus validating the approach used. Similarly, amplification products containing the termini expected for the (+) sgRNAs 1 to 5 were only observed in the PK-pretreated aliquots, confirming with a second independent approach the data from primer extensions and unveiling the presence of 5′-OH in these termini (Figure 5).

The previous results strongly suggested that the (+) sgRNAs are cleavage products and, accordingly, that their other terminal group was a 3′-P. To verify that this was indeed the case, we applied a 3′-RACE strategy. Two aliquots of the purified (+) sgRNAs 1 to 5 and of a full-length PSTVd (+) RNA control delimited by positions U179-U180—obtained by *in vitro* transcription and, therefore, with 5′-triphosphorylated and 3′-OH termini—were polyadenylated with yeast poly(A) polymerase, which catalyzes incorporation of AMP residues (from ATP) to 3′-OH terminal groups. The first aliquot remained untreated, while the second was pretreated with AP to remove phosphoryl groups from 3′-P termini. The polyadenylated products were reverse transcribed with a poly(A) tail-complementary primer (consisting of a 5′ moiety of 22 nt followed by 17 Ts ending with a degenerated A, C or G residue), PCR-amplified with this same primer and PSTVd-specific primers derived from the (+) sgRNAs 1 to 5 (Supplementary Table S3), fractionated by non-denaturing PAGE, and those of the expected size cloned and sequenced. As anticipated, the amplification product containing the termi-

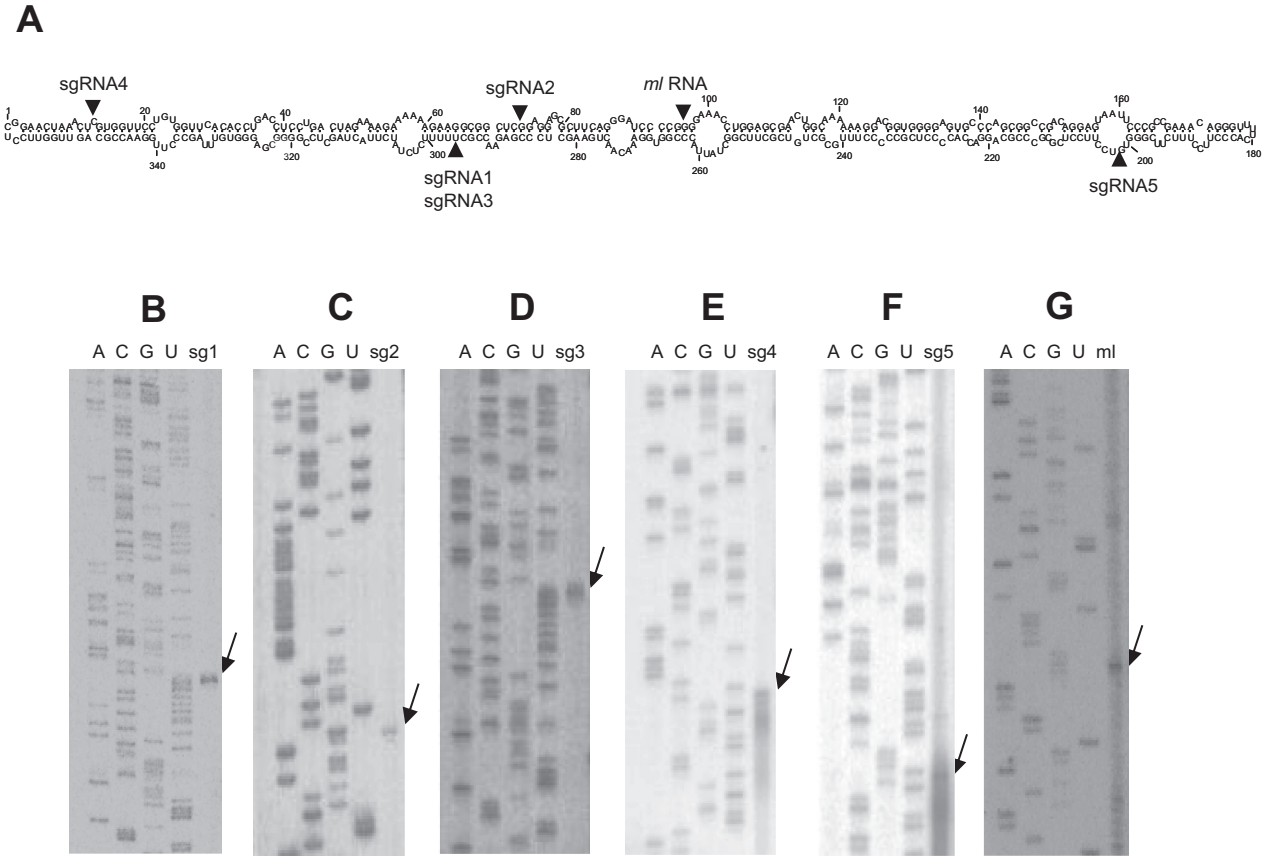

Figure 4. **(A)** Primer extension analysis of five PSTVd (+) sgRNAs and of the *ml* form reveals a complex population of 5′ termini (marked by arrowheads) mapping at different domains of the secondary structure of the genomic (+) viroid RNA predicted by Mfold (http://mfold.rna.albany.edu/?q=mfold/rna-folding-form) and supported by structural/functional analysis of a slightly different strain (48). Notice, however, that the 5′ termini of the (+) sgRNAs 1 and 3 map at the same position (U296). **(B–G)** Representative examples of extensions using primers RF-1242 (for sgRNAs 1 and 2, and for the *ml* form), RF-1194 (for sgRNAs 3 and 4) and RF-1191 (for sgRNA 5). In the six panels the sequencing ladders were obtained with the same primers and a recombinant plasmid containing a monomeric PSTVd-cDNA insert of the same variant (NB) used for inoculation. Arrows point to cDNA bands corresponding to 5′ termini.

nus predicted for the PSTVd (+) *ml* forms was observed regardless of the AP pretreatment. Yet, amplification products containing the termini expected for the (+) sgRNAs 1 to 5—according with their size and 5′-termini previously determined—were only detected in the AP-preteated aliquots, disclosing the presence of 3′-P in these termini (Supplementary Figure S5 and data not shown). The 3′-P termini of the (+) sgRNAs 1 to 5 were mapped at positions U178, C248, C94, C103 and C273, respectively, suggesting the participation of a pyrimidine-specific RNase in their genesis.

Overall, these results showed that the PSTVd (+) sgRNAs: (i) do not have a common 5′ terminus and, consequently, do not result from aborted transcription initiated at one specific site, and (ii) do have free 5′-OH and 3′-P termini most likely generated by one or more endoRNase producing these termini, and not by DCL or RISC that give rise to 5′-P and 3′-OH termini. A schematic mapping of the PSTVd (+) sgRNAs 1 to 5 on the secondary structure of the *mc* (+) form is presented below.

PSTVd (+) sgRNAs accumulate in the nucleus and most likely derive from cleavage of replicative intermediates

To gain an understanding of the potential substrate(s) giving rise to the PSTVd (+) sgRNAs, we examined their subcellular accumulation site and, particularly, whether this site was the nucleus wherein PSTVd replication takes place. Because preliminary experiments showed that obtaining nuclei preparations from *N. benthamiana* was much easier than from eggplant, we focused on the former host in which, even if the titer of PSTVd (+) sgRNAs is lower, still is sufficient to be detected (Figure 3). After confirming by DAPI staining and fluorescence microscopy the presence of nuclei in our preparations (data not shown), their RNA composition was compared with that of an equivalent amount of total RNAs by denaturing PAGE and northern-blot hybridization with a radioactive riboprobe for detecting PSTVd (+) strands. The resulting profiles were essentially identical, thus showing that the nucleus is the preferential accumulation site of the PSTVd (+) *mc* and linear *(ml)* genomic forms, in agreement with previous results (22,56), and, interestingly, also of the PSTVd (+) sgRNAs (Supplementary Figure S6). This observation, in conjunction with the finding that the 5′ ter-

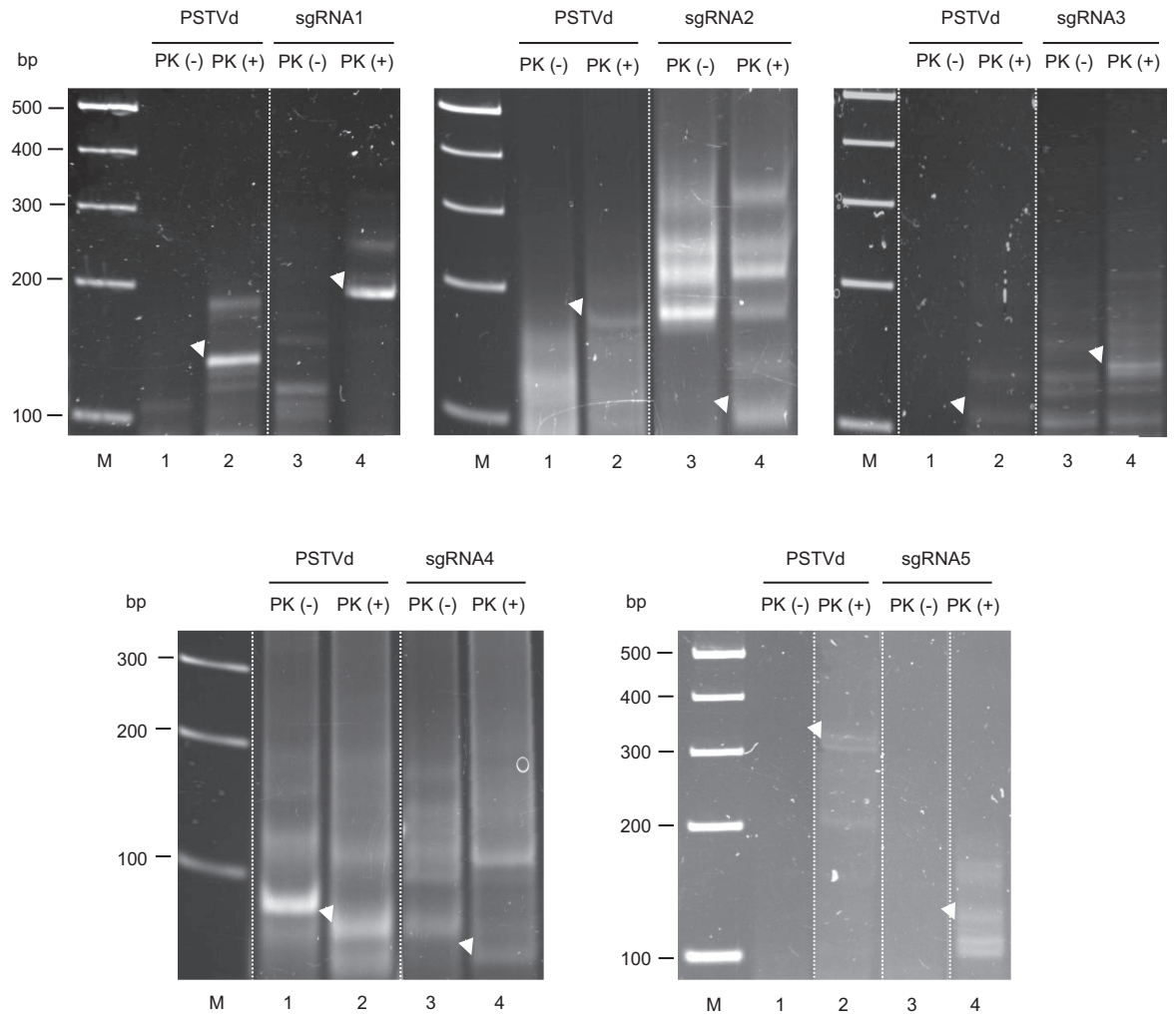

Figure 5. RLM-RACE analysis of the 5′ termini of the PSTVd (+) sgRNAs 1 to 5, using as control a PSTVd (+) *ml* form with 5′-hydroxyl (G2) and 2′,3′-cyclic phosphodiester (C1) termini resulting from ribozyme-mediated self-cleavage. Prior to RLM-RACE (see Supplementary Table S3 for the RNA adaptor and primers used), aliquots of each RNA were left untreated (lanes 1 and 3) or treated with PK and ATP to phosphorylate 5′-hydroxyl groups (lanes 2 and 4), with the resulting amplification products being then separated by non-denaturing PAGE and stained with ethidium bromide. Arrowheads indicate the amplicons of expected length that were eluted, cloned and sequenced. Lane M, DNA markers.

mini of the (+) sgRNAs do not map preferentially at loops in the rod-like secondary structure of the circular PSTVd (+) RNA (Figure 4)—in contrast with what would be expected if the latter were the substrate of the former—and also together with the detection of PSTVd (−) sgRNAs in infected tissue (see next section), is consistent with the sgRNAs being generated from replicative intermediates during their synthesis in the nucleus.

PSTVd (−) sgRNAs also accumulate in infected eggplant

To get a more comprehensive view, we finally examined the existence of PSTVd (−) sgRNAs. Because of the high self-complementarity of viroid RNAs, and because PSTVd (−) strands accumulate in infected tissue to significant lower amounts than their (+) counterparts (6), detection by northern-blot hybridization of the former in the presence of a vast excess of the latter posed a potential problem. Therefore, we chose highly restrictive conditions (50% formamide and 70°C) and confirmed that, under such conditions, radiolabeled PSTVd full-length riboprobes of each polarity hybridized only with their complementary unlabeled strand, and not with that of the same polarity (Figure 6). Moreover, while the *mc* and *ml* (+) forms were clearly visible in PSTVd-infected eggplant, no signals were observed in the position expected for the *mc* and *ml* (−) forms; this result is in agreement with previous data showing that these latter forms do not accumulate in infected tomato, wherein the prevalent (−) strands are multimeric (6,7). However, a pattern of PSTVd (−) sgRNAs, weaker in intensity and different in size from that of PSTVd (+) sgRNAs, was reproducibly detected (Figure 6).

Following the same approach described above, three PSTVd (−) sgRNAs (1 to 3) were gel-eluted (1 and 2 together because they appear as a doublet) and checked for purity by denaturing PAGE and northern-blot hybridization with a complementary full-length riboprobe (Supplementary Figure S7). The sgRNAs were then used as tem-

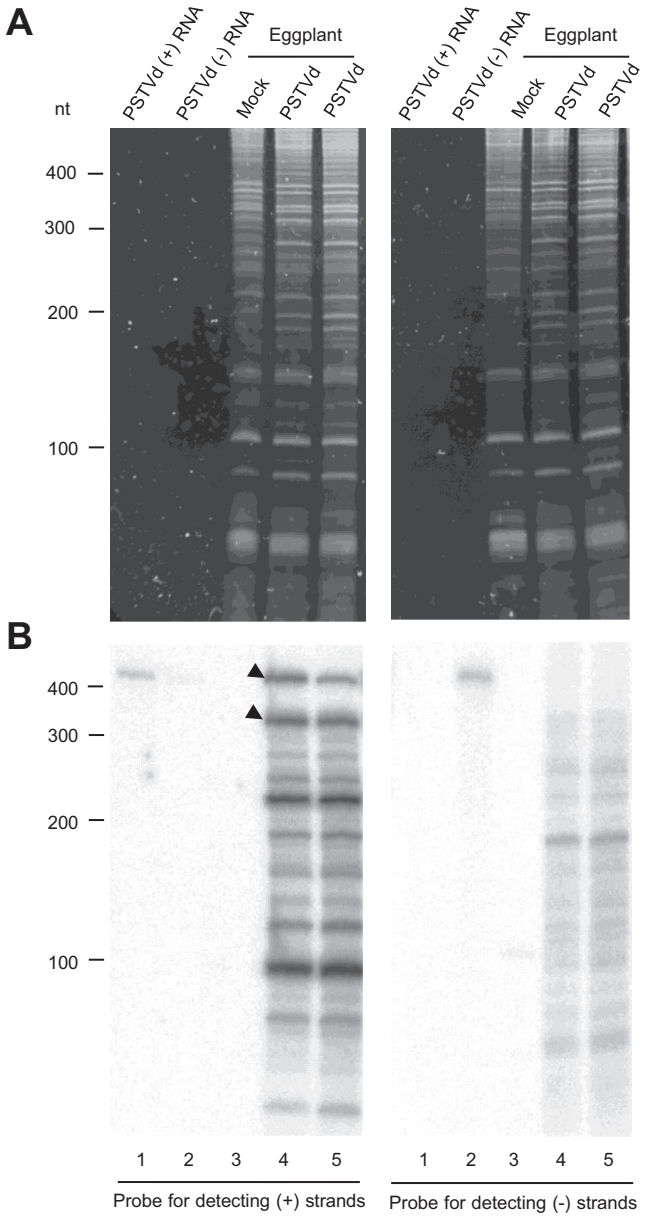

Figure 6. Infection of eggplant by PSTVd also results in the accumulation of a series of PSTVd (−) sgRNAs. Total RNAs from upper non-inoculated leaves collected at 20 dpi were separated by denaturing PAGE in 5% gels and revealed with ethidium bromide **(A),** and by northern-blot hybridization with full-length radiolabeled riboprobes (equalized in acid-precipitable counts) for detecting PSTVd (+) or (−) strands **(B)**. In each panel lanes 1 and 2 correspond to equal amounts of full-length PSTVd (+) and (−) transcripts, respectively (in both cases with 5′ and 3′ plasmid tails), lanes 3 to mock-inoculated eggplant, and lanes 4 and 5 to PSTVd-infected eggplant. Positions of the PSTVd (+) *mc* and ml forms are indicated with arrowheads and those of RNA markers (in nt) on the left.

plates for reverse transcriptase-mediated extensions with two 5′-radiolabeled primers each, and analyzed in parallel gel lanes with the sequencing ladders generated with the same primers. Examination of the autoradiograms revealed the C128, C156 and U159 as the 5′ termini for the (−) sgRNAs 1, 2 and 3, respectively (Figure 7), again showing the lack of a common 5′ terminus. Further characterization of the most abundant PSTVd (−) sgRNAs 3 via 5′- and 3′-RACE (Supplementary Figure S8) and subsequent cloning and sequencing as reported above, revealed a size of 184 nt consistent with that estimated from denaturing PAGE (Supplementary Figure S7), as well as 5′-OH (U159) and 3′-P (C335) termini, thus supporting the involvement in their genesis of a mechanism similar to that proposed for the PSTVd (+) sgRNAs. A schematic mapping of the PSTVd (+) sgRNAs 1 to 5 on the secondary structure of the *mc* (+) form, and of the PSTVd (−) sgRNAs 1 to 3 on the secondary structure of the *mc* (−) form, is presented in Figure 8.

DISCUSSION

The sgRNAs, which appear together with those of genomic size in infections by many positive-strand RNA viruses, serve usually for expressing viral proteins (57,58). However, this cannot be the role played by sgRNAs resulting from infection by viroids, because they are non-protein-coding RNAs. Previously, sgRNAs of both polarities have been found in association with two members of the family *Avsunviroidae*. More explicitly, in avocado infected by avocado sunblotch viroid (ASBVd) (59), viroid (+) and (−) sgRNAs of 137 and about 148 nt, respectively, were detected. Their 5′ termini are identical to those produced in the *in vitro* self-cleavage of dimeric (+) and (−) ASBVd strands, while their 3′ counterparts could represent sites of premature termination because, at least that of the ASBVd (+) sgRNA is not phosphorylated (9). On the other hand, in peach infected by peach latent mosaic viroid (PLMVd) (60), viroid (+) and (−) sgRNAs were also reported (44,61). Analyses of both sgRNAs regarding their size (about 240 nt) and 5′ termini (a triphosphorylated group), strongly support that they result from initiation at specific sites in each polarity strand and subsequent self-cleavage at the sites predicted by the corresponding hammerhead structures (before the first replication round was completed) (44). Therefore, the ASBVd and PLMVd sgRNAs have different origins: their 5′ termini mark the self-cleavage sites in the former and the transcription initiation sites in the latter.

Inspired by these findings, we assumed that molecular characterization of the PSTVd (+) sgRNAs accumulating reproducibly in infected eggplant could open a window on viroid dynamics *in vivo*. The observation of a similar, albeit weaker, profile of (+) sgRNAs in PSTVd-infected tomato and *N. benthamiana* strengthened our conviction that they were not artifacts generated *in vitro* during extraction, further reinforced by their absence in nucleic acid preparations from non-infected eggplant spiked with purified PSTVd *mc* forms. In principle, the PSTVd (+) sgRNAs could either be products of premature transcription termination, or result from endonucleolytic cleavage of longer viroid RNAs—either during replication or once it is completed—catalyzed by one or more RNases.

A first examination of nucleic acids from PSTV-infected eggplant by denaturing PAGE and northern-blot hybridization with six probes revealed that the (+) sgRNAs come from different regions of the genomic PSTVd (+) RNA. Subsequent primer extension analyses of five (+) sgRNAs showed the lack of a common 5′ terminus, dismissing the

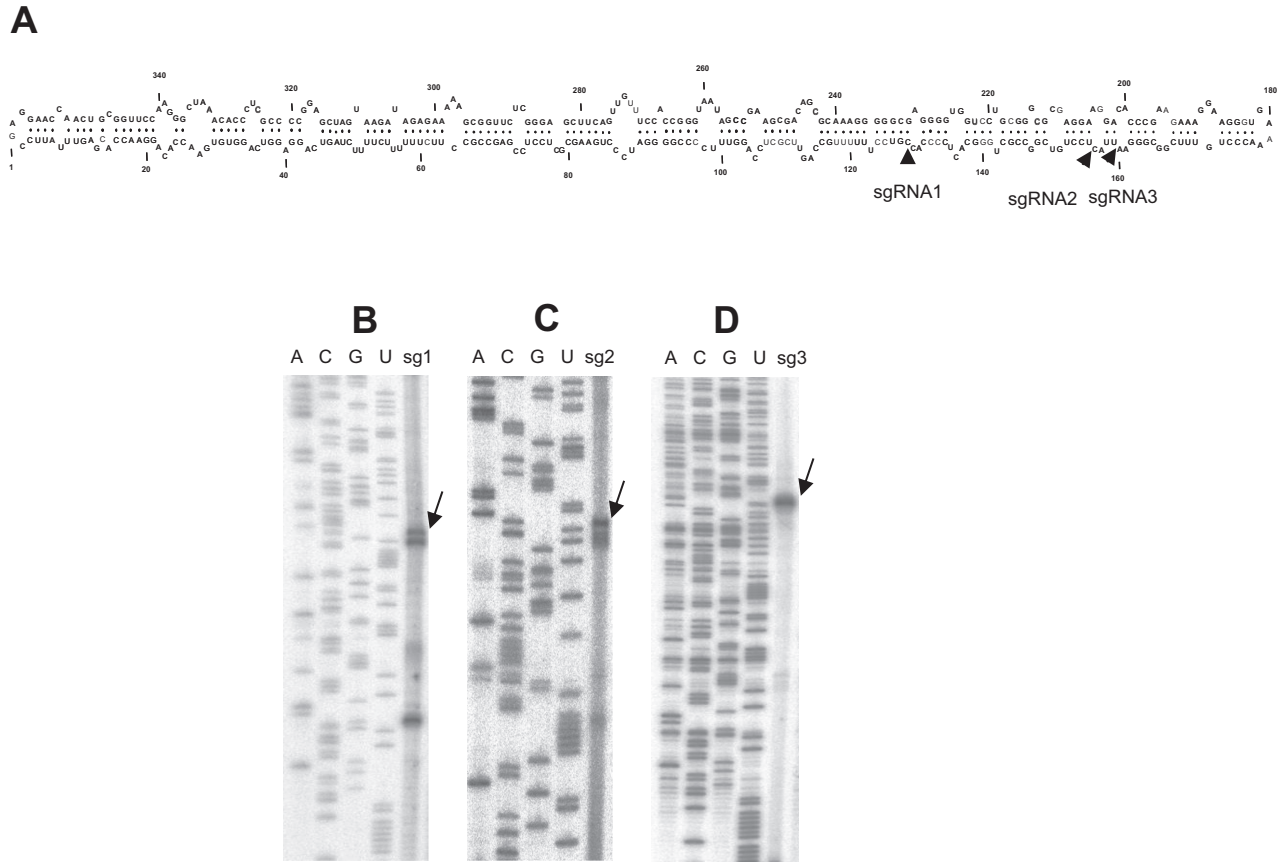

Figure 7. **(A)** Primer extension analysis of three PSTVd (−) sgRNAs showing their 5′ termini (marked by arrowheads) mapping at different positions on the secondary structure of the genomic (−) viroid RNA predicted by Mfold and validated by temperature-gradient gel electrophoresis .

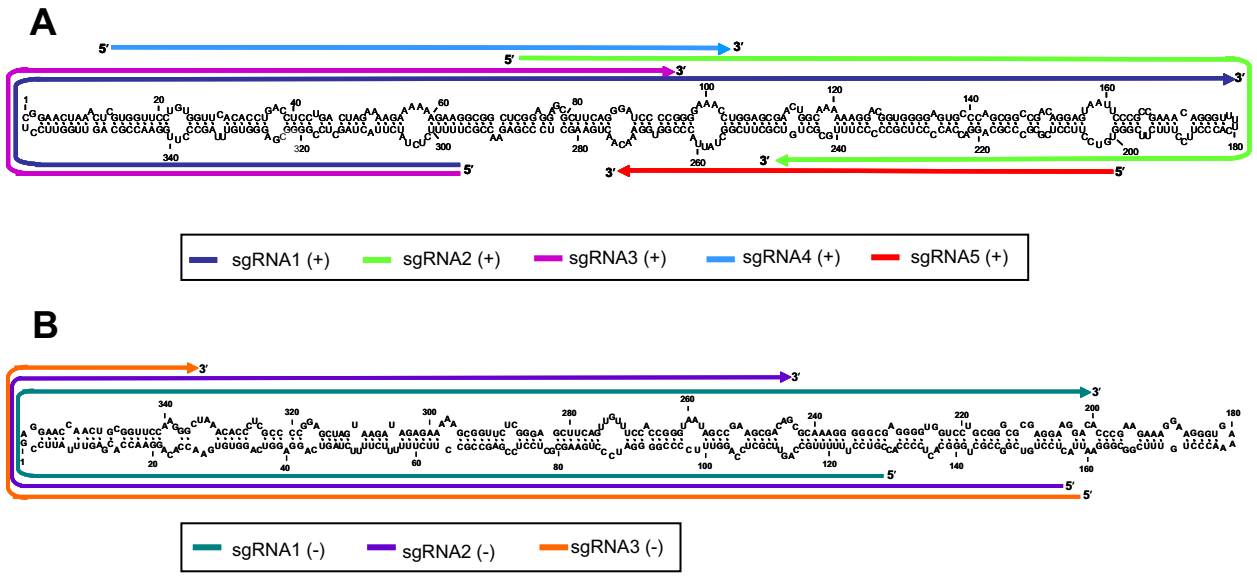

Figure 8. Schematic mapping of the PSTVd (+) sgRNAs 1 to 5 and of the (−) sgRNAs 1 to 3 on the genomic PSTVd (+) **(A)** and (−) **(B)** secondary structures, respectively. For easier comparison, the PSTVd (−) form is presented as a circular form, although this form has not been detected in infected tissue (7). The size of (+) sgRNAs 1 to 5 (242, 177, 158, 91 and 73 nt, respectively), and of the (−) sgRNAs 3 (184 nt), has been accurately determined by primer extension and 5′- and 3′-RACE; the size of the (−) sgRNAs 1 and 2 (285 and 280 nt) has been inferred from primer extension and mobility on denaturing PAGE, and is only approximate. Notice that the 5′ termini of the (+) sgRNAs 1 and 3 are coincidental, and that cleavage of the former at a specific site would generate the latter. Numbering in the (−) polarity is the same as in the (+) polarity.

possibility that they could result from aborted transcription initiated at one specific site, which if existing, should have a triphosphorylated or a capped group. Further supporting this view, 5′- and 3′-RACE experiments indicated that the (+) sgRNAs have 5′-OH and 3′-P termini most likely resulting from RNase-mediated endonucleolytic cleavage of longer viroid RNAs. Application of this methodology to the other polarity strand unveiled the accumulation of some PSTVd (−) sgRNAs with structural features similar to their (+) counterparts, thus leading to similar conclusions about their origin.

Studies like those reported here have been most likely disregarded so far by implicitly assuming that degradative pathways operating on viroid RNAs should generate heterogeneous products difficult to characterize. Our results show that this is not necessarily the case and that, by choosing the proper viroid-host combination, dissection of decay pathways—which together with biosynthesis determine the final RNA accumulation levels *in vivo*—becomes experimentally tractable and provides a fresh and intriguing insight into viroid turnover. More specifically, PSTVd degradation pathways appear to operate in an ordered and maybe even hierarchical manner. Why PSTVd sgRNAs of both polarities accumulate to higher levels in eggplant than in *N. benthamiana* and tomato remains a conundrum. These RNAs could be more stable in eggplant due to less active exonucleases; pertinent to this respect is the observation that the band pattern of total RNA preparations revealed by denaturing PAGE and ethidium bromide staining is more complex and intense in eggplant than in *N. benthamiana* and tomato (Figure 3A). Alternatively, or concurrently, the endoRNases involved in the genesis of the PSTVd sgRNAs, which presumably are enzymes developmentally regulated (62), could be more active in eggplant, particularly at early stages of viroid replication. In this context, two classes of plant endoRNases, I and II, have been described generating 3′-P termini (62).

Directly connected with these nucleolytic enzymes are their substrates. According to previous data from *in situ* hybridization (22), at least two PSTVd pools can be envisaged: one in the nucleoplasm, where elongation of viroids strands of both polarities occurs, and the other in the nucleolus, where only (+) polarity strands are processed, with the endoRNases present in both subnuclear compartments being most likely different. The finding of PSTVd sgRNAs of both polarities suggests that they are generated in the nucleoplasm during polymerization of viroid strands, a notion consistent with the nuclear accumulation of the PSTVd (+) sgRNAs in *N. benthamiana.* This view is further supported by the higher levels of the (+) PSTVd-sgRNAs detected in the agroinfiltrated leaves of *N. benthamiana* (wherein an earlier and more synchronous infection is established) than in the upper non-inoculated leaves. The most direct interpretation for this observation is that a significant part of the PSTVd (+) sgRNAs results from cleavage of the primary PSTVd (+) dimeric transcript, which mimics a replicative intermediate. Previous data obtained with transgenic *Arabidopsis thaliana* expressing dimeric (+) transcripts of two PSTVd-related viroids have shown that these transcripts are indeed recognized and processed as replicative intermediates (63). Moreover, since most RNases generating 5′-OH and 3′-P termini, like pancreatic RNase (64), have a preference for single-stranded regions and we have not observed the 5′ termini of the PSTVd (+) sgRNAs mapping preferentially at loops in the rod-like secondary structure of the *mc* (+) form, this RNA does not appear a plausible precursor. There is solid evidence supporting the existence and function—in replication and, particularly, in movement—of some of these loops (48,65–66); yet, a significant fraction of the *mc* (+) form may function as a reservoir molecule, most likely interacting *in vivo* with host proteins that protect its structure and make it less accessible to RNases. On the other hand, detection of PSTVd (−) sgRNAs is consistent with their coming from endonucleolytic cleavage of nascent (−) strands, because the strands of this polarity forming part of replicative intermediates or replicative forms should be less sensitive to endoRNases with preference for single-stranded RNAs.

In closing, viroid RNA turnover raises specific questions because, in contrast to RNA viruses whose genome is protected by a capsid protein, viroid genomes are naked RNAs more vulnerable to endoRNases (but not to exonucleases due to their circular structure). Moreover, while replication of RNA viruses occurs in organelle-associated membranous vesicles connected with the cytoplasm (67), that of PSTVd and other representative members of its family takes place in the nucleus (22,56,68). Our results provide a novel insight on a complementary pathway: how viroid decay may proceed *in vivo*, possibly during replication. The pathway here reported, combined with others based on RNA silencing that could target double-stranded replicative intermediates or the *mc* (+) form during its movement, would ultimately counteract synthesis of viroid strands, thus finely tuning their final accumulation in infected tissues. The possibility that synthesis and decay of PSTVd strands might be coupled—somehow resembling the situation observed in mRNA—cannot be excluded, particularly considering that transcription is mediated by RNA polymerase II in both cases.

SUPPLEMENTARY DATA

Supplementary Data are available at NAR Online.

ACKNOWLEDGEMENTS

We are grateful to A. Ahuir for excellent technical assistance, and to Drs J. A. Daròs, M. de la Peña and C. Hernández for valuable suggestions or materials.

FUNDING

Ministerio de Economía y Competitividad (MINECO) [BFU2011-28443 to R. F. laboratory]; MINECO [to S.M. and S.D.]. Funding for open access charge: MINECO (BFU2011-28443 to R.F.); Ministero dell'Economia e Finanze Italiano to the CNR (CISIA, Legge 191/2009 to B.N. and F.D.S.).
Conflict of interest statement. None declared.

REFERENCES

1. Diener,T.O. (2003) Discovering viroids—a personal perspective. *Nat. Rev. Microbiol.*, **1**, 75–80.

2. Tabler,M. and Tsagris,M. (2004) Viroids: petite RNA pathogens with distinguished talents. *Trends Plant Sci.*, **9**, 339–348.
3. Flores,R., Hernández,C., Martínez de Alba,A.E., Daròs,J.A. and Di Serio,F. (2005) Viroids and viroid-host interactions. *Annu. Rev. Phytopathol.*, **43**, 117–139.
4. Ding,B. (2009) The biology of viroid-host interactions. *Annu. Rev. Phytopathol.*, **47**, 105–131.
5. Ishikawa,M., Meshi,T., Ohno,T., Okada,Y., Sano,T., Ueda,I. and Shikata,E. (1984) A revised replication cycle for viroids: the role of longer than unit RNA in viroid replication. *Mol. Gen. Gen.*, **196**, 421–428.
6. Branch,A.D., Benenfeld,B.J. and Robertson,H.D. (1988) Evidence for a single rolling circle in the replication of potato spindle tuber viroid. *Proc. Natl. Acad. Sci. U.S.A.*, **85**, 9128–9132.
7. Feldstein,P.A., Hu,Y. and Owens,R.A. (1998) Precisely full length, circularizable, complementary RNA: an infectious form of potato spindle tuber viroid. *Proc. Natl. Acad. Sci. U.S.A.*, **95**, 6560–6565.
8. Hutchins,C., Rathjen,P.D., Forster,A.C. and Symons,R.H. (1986) Self-cleavage of plus and minus RNA transcripts of avocado sunblotch viroid. *Nucleic Acids Res.*, **14**, 3627–3640.
9. Daròs,J.A., Marcos,J.F., Hernández,C. and Flores,R. (1994) Replication of avocado sunblotch viroid: evidence for a symmetric pathway with two rolling circles and hammerhead ribozyme processing. *Proc. Natl. Acad. Sci. U.S.A.*, **91**, 12813–12817.
10. Flores,R., Daròs,J.A. and Hernández,C. (2000) The *Avsunviroidae* family: viroids with hammerhead ribozymes. *Adv. Virus Res.*, **55**, 271–323.
11. Diener,T.O. (1971) Potato spindle tuber 'virus': IV. A replicating, low molecular weight RNA. *Virology*, **45**, 411–428.
12. Sänger,H.L., Klotz,G., Riesner,D., Gross,H.J. and Kleinschmidt,A. (1976) Viroids are single-stranded covalently closed circular RNA molecules existing as highly base-paired rod-like structures. *Proc. Natl. Acad. Sci. U.S.A.*, **73**, 3852–3856.
13. Gross,H.J., Domdey,H., Lossow,C., Jank,P., Raba,M., Alberty,H. and Sänger,H.L. (1978) Nucleotide sequence and secondary structure of potato spindle tuber viroid. *Nature*, **273**, 203–208.
14. Owens,R.A. (2007) Potato spindle tuber viroid: the simplicity paradox resolved? *Mol. Plant Pathol.*, **8**, 549–560.
15. Mühlbach,H.P. and Sänger,H.L. (1979) Viroid replication is inhibited by α-amanitin. *Nature*, **278**, 185–188.
16. Flores,R. and Semancik,J.S. (1982) Properties of a cell-free system for synthesis of citrus exocortis viroid. *Proc. Natl. Acad. Sci. U.S.A.*, **79**, 6285–6288.
17. Schindler,I.M. and Mühlbach,H.P. (1992) Involvement of nuclear DNA-dependent RNA polymerases in potato spindle tuber viroid replication: a reevaluation. *Plant Sci.*, **84**, 221–229.
18. Warrilow,D. and Symons,R.H. (1999) Citrus exocortis viroid RNA is associated with the largest subunit of RNA polymerase II in tomato in vivo. *Arch. Virol.*, **144**, 2367–2375.
19. Gas,M.E., Hernández,C., Flores,R. and Daròs,J.A. (2007) Processing of nuclear viroids *in vivo:* an interplay between RNA conformations. *PLoS Pathog.*, **3**, 1813–1826.
20. Gas,M.E., Molina-Serrano,D., Hernández,C., Flores,R. and Daròs,J.A. (2008) Monomeric linear RNA of citrus exocortis viroid resulting from processing *in vivo* has 5′-phosphomonoester and 3′-hydroxyl termini: implications for the ribonuclease and RNA ligase involved in replication. *J. Virol.*, **82**, 10321–10325.
21. Nohales,M.A., Flores,R. and Daròs,J.A. (2012) Viroid RNA redirects host DNA ligase 1 to act as an RNA ligase. *Proc. Natl. Acad. Sci. U.S.A.*, **109**, 13805–13810.
22. Qi,Y. and Ding,B. (2003) Differential subnuclear localization of RNA strands of opposite polarity derived from an autonomously replicating viroid. *Plant Cell*, **15**, 2566–2577.
23. Lewis,J.D. and Tollervey,D. (2000) Like attracts like: getting RNA processing together in the nucleus. *Science*, **288**, 1385–1389.
24. Dori-Bachash,M., Shema,E. and Tirosh,I. (2011) Coupled evolution of transcription and mRNA degradation. *PLoS Biol.*, **9**, e1001106.
25. Pérez-Ortín,J.E., Alepuz,P., Chávez,S. and Choder,M. (2013) Eukaryotic mRNA decay: methodologies, pathways, and links to other stages of gene expression. *J. Mol. Biol.*, **425**, 3750–3775.
26. Haimovich,G., Medina,D.A., Causse,S.Z., Garber,M., Millán-Zambrano,G., Barkai,O., Chávez,S., Pérez-Ortín,J.E., Darzacq,X. and Choder,M. (2013) Gene expression is circular: factors for mRNA degradation also foster mRNA synthesis. *Cell*, **153**, 1000–1011.
27. Papaefthimiou,I., Hamilton,A.J., Denti,M.A., Baulcombe,D.C., Tsagris,M. and Tabler,M. (2001) Replicating potato spindle tuber viroid RNA is accompanied by short RNA fragments that are characteristic of post-transcriptional gene silencing. *Nucleic Acids Res.*, **29**, 2395–2400.
28. Itaya,A., Folimonov,A., Matsuda,Y., Nelson,R.S. and Ding,B. (2001) Potato spindle tuber viroid as inducer of RNA silencing in infected tomato. *Mol. Plant Microbe Interact.*, **14**, 1332–1334.
29. Martínez de Alba,A.E., Flores,R. and Hernández,C. (2002) Two chloroplastic viroids induce the accumulation of the small RNAs associated with post-transcriptional gene silencing. *J. Virol.*, **76**, 13094–13096.
30. Navarro,B., Gisel,A., Rodio,M.E., Delgado,S., Flores,R. and Serio,F. (2012) Viroids: how to infect a host and cause disease without encoding proteins. *Biochimie*, **94**, 1474–1480.
31. Hammann,C. and Steger,G. (2012) Viroid-specific small RNA in plant disease. *RNA Biol.*, **9**, 809–819.
32. Bernstein,E., Caudy,A.A., Hammond,S.M. and Hannon,G.J. (2001) Role for a bidentate ribonuclease in the initiation step of RNA interference. *Nature*, **409**, 363–366.
33. Qi,Y., Denli,A.M. and Hannon,G., J. (2005) Biochemical specialization within Arabidopsis RNA silencing pathways. *Mol. Cell*, **19**, 421–428.
34. Minoia,S., Carbonell,A., Di Serio,F., Gisel,A., Carrington,J.C., Navarro,B. and Flores,R. (2014) Specific ARGONAUTES bind selectively small RNAs derived from potato spindle tuber viroid and attenuate viroid accumulation in vivo. *J. Virol.*, **88**, 11933–11945.
35. Bohmert,K., Camus,I., Bellini,C., Bouchez,D., Caboche,M. and Benning,C. (1998) AGO1 defines a novel locus of Arabidopsis controlling leaf development. *EMBO J.*, **17**, 170–180.
36. Hammond,S.M., Bernstein,E., Beach,D. and Hannon,G.J. (2000) An RNA-directed nuclease mediates post-transcriptional gene silencing in Drosophila cells. *Nature*, **404**, 293–296.
37. Mallory,A. and Vaucheret,H. (2010) Form, function, and regulation of ARGONAUTE proteins. *Plant Cell*, **22**, 3879–3889.
38. Matousek,J., Kozlová,P., Orctová,L., Schmitz,A., Pesina,K., Bannach,O., Diermann,N., Steger,G. and Riesner,D. (2007) Accumulation of viroid-specific small RNAs and increase in nucleolytic activities linked to viroid-caused pathogenesis. *Biol. Chem.*, **388**, 1–13.
39. Matousek,J., Orctová,L., Skopek,J., Pesina,K. and Steger,G. (2008). Elimination of hop latent viroid upon developmental activation of pollen nuclease. *Biol. Chem.*, **389**, 905–918.
40. Grimsley,N., Hohn,B., Hohn,T. and Walden,R. (1986) Agroinfection, an alternative route for viral-infection of plants by using the Ti plasmid. *Proc. Natl. Acad. Sci. U.S.A.*, **83**, 3282–3286.
41. Sambrook,J., Fritsch,E.F. and Maniatis,T. (1989) *Molecular Cloning: A Laboratory Manual*, 2nd edn, Cold Spring Harbor Laboratory Press, Cold Spring Harbor, NY.
42. Di Serio,F., Martínez de Alba,A.E., Navarro,B., Gisel,A. and Flores,R. (2010) RNA-dependent RNA polymerase 6 delays accumulation and precludes meristem invasion of a nuclear-replicating viroid. *J. Virol.*, **84**, 2477–2489.
43. Carbonell,A., Flores,R. and Gago,S. (2011) *Trans*-cleaving hammerhead ribozymes with tertiary stabilizing motifs: *in vitro* and *in vivo* activity against a structured viroid RNA. *Nucleic Acids Res.*, **39**, 2432–2444.
44. Delgado,S., Martínez de Alba,A.E., Hernández,C. and Flores,R. (2005) A short double-stranded RNA motif of peach latent mosaic viroid contains the initiation and the self-cleavage sites of both polarity strands. *J. Virol.*, **79**, 12934–12943.
45. Sikorskaite,S., Rajamäki,M.L., Baniulis,D., Stanys,V. and Valkonen,J.P.T. (2013) Protocol: Optimised methodology for isolation of nuclei from leaves of species in the Solanaceae and Rosaceae families. *Plant Meth.*, **9**, 31.
46. Raymer,W.B. and O'Brien,M.J. (1962) Transmission of potato spindle tuber virus to tomato. *Am. Potato J.*, **39**, 401–408.
47. Qi,Y. and Ding,B. (2002) Replication of potato spindle tuber viroid in cultured cells of tobacco and *Nicotiana benthamiana:* the role of specific nucleotides in determining replication levels for host adaptation. *Virology*, **302**, 445–456.

48. Zhong,X., Archual,A.J., Amin,A.A. and Ding,B. (2008) A genomic map of viroid RNA motifs critical for replication and systemic trafficking. *Plant Cell*, **20**, 35–47.
49. Yang,S.J., Carter,S.A., Cole,A.B., Cheng,N.H. and Nelson,R.S. (2004) A natural variant of a host RNA-dependent RNA polymerase is associated with increased susceptibility to viruses by *Nicotiana benthamiana*. *Proc. Natl. Acad. Sci. U.S.A.*, **101**, 6297–6302.
50. Goodin,M.M., Zaitlin,D., Naidu,R.A. and Lommel,S.A. (2008) *Nicotiana benthamiana:* its history and future as a model for plant-pathogen interactions. *Mol. Plant Microbe Interact.*, **21**, 1015–1026.
51. O'Brien,M.J. (1972) Hosts of potato spindle tuber virus in suborder *Solanineae*. *Am. Potato J.*, **49**, 70–72.
52. Fadda,Z., Daròs,J.A., Fagoaga,C., Flores,R. and Duran-Vila,N. (2003) Eggplant latent viroid (ELVd): candidate type species for a new genus within family *Avsunviroidae* (hammerhead viroids). *J. Virol.*, **77**, 6528–6532.
53. Markarian,N., Li,H.W., Ding,S.W. and Semancik,J.S. (2004) RNA silencing as related to viroid induced symptom expression. *Arch. Virol.*, **149**, 397–406.
54. Carbonell,A., Martínez de Alba,A.E., Flores,R. and Gago,S. (2008) Double-stranded RNA interferes in a sequence-specific manner with infection of representative members of the two viroid families. *Virology*, **371**, 44–53.
55. Baumstark,T., Schröder,A.R. and Riesner,D. (1997) Viroid processing: switch from cleavage to ligation is driven by a change from a tetraloop to a loop E conformation. *EMBO J.*, **16**, 599–610.
56. Harders,J., Lukacs,N., Robert-Nicoud,M., Jovin,J.M. and Riesner,D. (1989) Imaging of viroids in nuclei from tomato leaf tissue by in situ hybridization and confocal laser scanning microscopy. *EMBO J.*, **8**, 3941–3949.
57. Miller,W.A. and Koev,G. (2000) Synthesis of subgenomic RNAs by positive-strand RNA viruses. *Virology*, **273**, 1–8.
58. Sztuba-Solinska,J., Stollar,V. and Bujarski,J.J. (2011) Subgenomic messenger RNAs: mastering regulation of (+)-strand RNA virus life cycle. *Virology*, **412**, 245–255.
59. Symons,R.H. (1981) Avocado sunblotch viroid: primary sequence and proposed secondary structure. *Nucleic Acids Res.*, **9**, 6527–6537.
60. Hernández,C. and Flores,R. (1992) Plus and minus RNAs of peach latent mosaic viroid self-cleave in vitro via hammerhead structures. *Proc. Natl. Acad. Sci. U.S.A.*, **89**, 3711–3715.
61. Pelchat,M., Côté,F. and Perreault,J.P. (2001) Study of the polymerization step of the rolling circle replication of peach latent mosaic viroid. *Arch. Virol.*, **146**, 1753–1763.
62. Green,P.J. (1994) The ribonucleases of higher plants. *Annu. Rev. Plant Physiol. Plant Mol. Biol.*, **45**, 421–445.
63. Daròs,J.A. and Flores,R. (2004) *Arabidopsis thaliana* has the enzymatic machinery for replicating representative viroid species of the family *Pospiviroidae*. *Proc. Natl. Acad. Sci. U.S.A.*, **101**, 6792–6797.
64. Cuchillo,C.M., Nogués,M.V. and Raines,R.T. (2011) Bovine pancreatic ribonuclease: fifty years of the first enzymatic reaction mechanism. *Biochemistry*, **50**, 7835–7841.
65. Zhong,X., Tao,X., Stombaugh,J., Leontis,N. and Ding,B. (2007) Tertiary structure and function of an RNA motif required for plant vascular entry to initiate systemic trafficking. *EMBO J.*, **26**, 3836–3846.
66. Takeda,R., Petrov,A.I., Leontis,N.B. and Ding,B. (2011) A three-dimensional RNA motif in potato spindle tuber viroid mediates trafficking from palisade mesophyll to spongy mesophyll in *Nicotiana benthamiana*. *Plant Cell*, **23**, 258–272.
67. den Boon,J.A. and Ahlquist,P. (2010) Organelle-like membrane compartmentalization of positive-strand RNA virus replication factories. *Annu. Rev. Microbiol.*, **64**, 241–56.
68. Bonfiglioli,R.G., Webb,D.R. and Symons,R.H. (1996) Tissue and intra-cellular distribution of coconut cadang-cadang viroid and citrus exocortis viroid determined by in situ hybridization and confocal laser scanning and transmission electron microscopy. *Plant J.*, **9**, 457–465.